

RecQ Helicase Stimulates Both DNA Catenation and Changes in DNA Topology by Topoisomerase III*

Received for publication, March 24, 2003, and in revised form, June 10, 2003
Published, JBC Papers in Press, August 8, 2003, DOI 10.1074/jbc.M302994200

Frank G. Harmon[‡], Joel P. Brockman, and Stephen C. Kowalczykowski[§]

From the Division of Biological Sciences, Sections of Microbiology and of Molecular and Cellular Biology, Center for Genetics and Development, University of California, Davis, California 95616

Together, RecQ helicase and topoisomerase III (Topo III) of *Escherichia coli* comprise a potent DNA strand passage activity that can catenate covalently closed DNA (Harmon, F. G., DiGate, R. J., and Kowalczykowski, S. C. (1999) *Mol. Cell* 3, 611–620). Here we directly assessed the structure of the catenated DNA species formed by RecQ helicase and Topo III using atomic force microscopy. The images show complex catenated DNA species involving crossovers between multiple double-stranded DNA molecules that are consistent with full catenanes. *E. coli* single-stranded DNA-binding protein significantly stimulated both the topoisomerase activity of Topo III alone and the DNA strand passage activity of RecQ helicase and Topo III. Titration data suggest that an intermediate of the RecQ helicase unwinding process, perhaps a RecQ helicase-DNA fork, is the target for Topo III action. Catenated DNA is the predominant product under conditions of molecular crowding; however, we also discovered that RecQ helicase and single-stranded DNA-binding protein greatly stimulated the intramolecular strand passage (“supercoiling”) activity of Topo III, as revealed by changes in the linking number of uncatenated DNA. Together our results demonstrate that RecQ helicase and Topo III function together to comprise a potent and concerted single-strand DNA passage activity that can mediate both catenation-decatenation processes and changes in DNA topology.

The RecQ family of proteins is a large and important class of DNA helicases (for review, see Ref. 1). Members of this helicase family are widespread, having been identified in bacteria (RecQ) (2), fungi (Sgs1, Rqh1, QDE3) (3–6), fly (Dmblm) (7), frog (FFA-1) (8), and humans (RECQL, BLM, WRN, RECQ4, and RECQ5) (9–12). These proteins share significant amino acid similarity within the seven characteristic helicase motifs (13), and they possess many common biochemical attributes (14–17). Because of the association of mutations in several of these proteins with human diseases, understanding the role of these RecQ-like helicases in DNA metabolism is likely to provide an important understanding of the molecular basis of these diseases. Null mutations in the WRN helicase are implicated in Werner’s syndrome, the major clinical manifestation of

which is premature aging and a predisposition to cancer (10). Loss of BLM helicase function results in Bloom’s syndrome; in this case, afflicted individuals are highly susceptible to certain types of cancer (15). Mutations in the RECQ4 helicase are found in a subset of Rothmund-Thompson syndrome cases, a disease that is also typified by a predisposition to malignancy (12, 18).

Phenotypic analysis indicates that these helicases are needed in their respective organisms to maintain the stability of the genome (for review, see Ref. 19). For example, human cells lacking BLM helicase function display elevated levels of sister chromatid exchange (20). Similarly, gross chromosomal rearrangements and breakage are common phenotypes of human cells lacking WRN helicase function. In the yeast *Saccharomyces cerevisiae*, *SGS1* mutation leads to genetic instability at the rDNA locus, which results in premature aging in this organism (3, 21, 22). Similarly, inactivation of the Rqh1 helicase in the fission yeast *Schizosaccharomyces pombe* leads to an increased incidence of chromosome nondisjunction and elevated levels of recombination following DNA damage (5). Furthermore, a null mutation at the *recQ* locus, which encodes the RecQ helicase from *Escherichia coli*, results in a 30-fold increase in illegitimate recombination (23).

Genomic stability in many organisms also appears to require the function of a Topo III¹-like enzyme. Similar to the RecQ family of helicases, these topoisomerases are highly conserved, with structural homologues identified in humans (24, 25), mouse (26), yeast (27), and bacteria (28). An indication of their importance in DNA metabolism is reflected in the fact that mammalian cells possess two distinct isoforms of Topo III, hTopo III α and hTopo III β . Furthermore, a null mutation in mouse Topo III α is embryonically lethal (26). Additionally, loss of Topo III function in *S. pombe* leads to aberrant mitotic chromosome segregation, and these effects are ultimately lethal (29, 30). In *S. cerevisiae*, *top3* mutants display elevated levels of homologous recombination between short repeated DNA sequences (27). Similarly, loss of Topo III function in *E. coli* results in an increase in deletions arising from recombination events between direct repeats (31, 32). Purification of the *E. coli* and *S. cerevisiae* proteins revealed that these topoisomerases also share several common biochemical attributes. Both the yeast and bacterial proteins are type 1A topoisomerases (*i.e.* binding and strand cleavage is limited to one strand);

* The costs of publication of this article were defrayed in part by the payment of page charges. This article must therefore be hereby marked “advertisement” in accordance with 18 U.S.C. Section 1734 solely to indicate this fact.

[‡] Present address: Dept. of Cell Biology, Scripps Research Inst., La Jolla, CA 92037.

[§] To whom correspondence should be addressed: Section of Microbiology, Briggs Hall, 1 Shields Ave., University of California, Davis, CA 95616. Tel.: 530-752-5938; Fax: 530-752-5939; E-mail: skowalczykowski@ucdavis.edu.

¹ The abbreviations used are: Topo III, topoisomerase III; ssDNA, single-stranded DNA; AFM, atomic force microscopy; scDNA, supercoiled DNA; rcDNA, relaxed, covalently closed DNA; PEG, polyethylene glycol; hdDNA, heat-denatured, relaxed, covalently closed DNA; K_{eff} , effective concentration of protein required to reach half the maximal rate of catenation; Topo I, topoisomerase I; wgTopo I, wheat germ topoisomerase I; ΔLk , linking number difference from relaxed DNA; scDNA, supercoiled DNA; SSB protein, single-stranded DNA-binding protein; ATP γ S, adenosine 5'-O-(thiotriphosphate).

therefore, each displays a distinct preference for acting on DNA substrates having regions of ssDNA (33, 34). Another common attribute of Topo III-like enzymes is that they more readily catenate/decatenate DNA molecules that possess ssDNA regions, whereas they remove supercoils from fully duplex DNA molecules slowly.

An emerging paradigm for the RecQ-like helicases is that their role in DNA metabolism requires a specific interaction between the helicase and a Topo III-like topoisomerase. This unusual functional pairing of proteins was first identified in *S. cerevisiae*, where a mutation in *SGS1* was found to suppress the hyper-recombination phenotype of *top3* mutants (3). In addition, epistasis analysis also indicated that *TOP3* and *SGS1* act in the same pathway. This was supported by the fact that Sgs1 physically interacts with yeast Topo III (3, 35). The *S. pombe* Rqh1 helicase and its cognate Topo III also share a genetic interaction, because a *rqh1* deletion suppresses the lethal phenotype of a *TOP3* mutation (29). Furthermore, the human BLM helicase physically interacts with hTopo III α (36) and, in a heterologous eukaryotic system, yeast Sgs1 helicase interacts with hTopo III β (25). Finally, the coupling of helicase and topoisomerase function was also identified in bacteria; *E. coli* RecQ helicase functionally interacts with *E. coli* Topo III *in vitro*, and a similar behavior was also observed for RecQ helicase and Topo III from *S. cerevisiae* (37). These findings were consistent with this being a conserved activity of RecQ-like helicases and Topo III-like topoisomerases.

The biochemical consequences of these interactions are largely unknown, except in the case of *E. coli* Topo III and RecQ helicase. Acting together, these two proteins exhibit a potent duplex DNA strand passage activity that is absent in either of the individual proteins. The DNA strand passage activity possessed by this combination of proteins is unique in that it permits Topo III to catenate and decatenate covalently closed duplex DNA (37). Recent work has also demonstrated that BLM helicase (in conjunction with human RPA) significantly stimulates the DNA strand passage activity of hTopo III (38).

Here we further characterized the DNA strand passage activity of RecQ helicase and Topo III with respect to the effects of ssDNA-binding proteins, the concentration of both RecQ helicase and Topo III, and the effect of macromolecular crowding. Furthermore, the structure of the catenated DNA produced by RecQ helicase and Topo III was visualized using AFM. We discovered that RecQ helicase and Topo III also can efficiently change the linking number of rcDNA, and we found that negative supercoils are exclusively introduced into covalently closed dsDNA. A mechanism for how RecQ helicase and Topo III promote such diverse reactions is proposed.

EXPERIMENTAL PROCEDURES

Reagents—Chemicals were reagent grade, and all solutions were prepared using Barnstead NanoPure water. PEG (M_r 8,000) was purchased from Sigma, dissolved in water as a 40% (w/v) stock, and used without further purification. Phosphoenolpyruvate and ATP were purchased from Sigma. Nucleotides were dissolved in water as concentrated stock solutions at pH 7.5 and the concentrations determined spectrophotometrically using an extinction coefficient of $1.54 \times 10^4 \text{ M}^{-1} \text{ cm}^{-1}$ at 260 nm. Chloroquine diphosphate was purchased from Sigma and was dissolved as a concentrated stock solution in water.

Proteins—RecQ helicase and RecA protein were purified as described previously (39). *E. coli* Topo III and Topo I were purified as described previously (33, 40). Wheat germ topoisomerase I was purchased from Promega. SSB protein was purified from *E. coli* strain RLM727 as described (41), and its concentration was determined as described previously (42). *S. cerevisiae* RPA was provided by Noriko Kantake (University of California, Davis, CA).

DNA—pUC19 supercoiled DNA (scDNA) was purified using alkaline lysis followed by CsCl-ethidium bromide equilibrium centrifugation (43). pUC19 rcDNA was produced by treatment of pUC19 scDNA with 1 unit of wheat germ Topo I/ μg of DNA, as described by the manufac-

turer. The relaxed dsDNA was recovered by ethanol precipitation, following phenol extraction. The molar nucleotide concentration of dsDNA was determined using an extinction coefficient of $6.5 \times 10^3 \text{ M}^{-1} \text{ cm}^{-1}$ at 260 nm. Topoisomers having a defined mean ΔLk value (from 0.01 to -8.0) were produced from pUC19 scDNA using wheat germ Topo I and ethidium bromide, using the method of Bowater *et al.* (44).

RecQ Helicase-Topo III Assays—All catenation reactions were carried out as described previously (37), with the indicated changes. Standard conditions consisted of 25 mM Tris acetate (pH 7.5), 10% PEG, 1 mM magnesium acetate, 0.1 mM dithiothreitol, 1 mM phosphoenolpyruvate, 80 units ml^{-1} pyruvate kinase, 0.1 mg ml^{-1} bovine serum albumin, and 1 mM ATP. Standard reactions were 50 μl and consisted of 15 μM (nucleotides: 5.6 nM molecules) pUC19 scDNA or rcDNA (as indicated), 1.0 μM SSB protein, 1.0 μM RecQ helicase, and 0.1 μM Topo III. When RPA was substituted for SSB protein, its concentration was 0.32 μM . Utilization of rcDNA substrate was determined from agarose gels stained with 0.5 $\mu\text{g}/\text{ml}$ ethidium bromide, using ImageQuant software (Amersham Biosciences).

The effect of SSB protein and RPA on the relaxation activity of Topo III was assayed under standard conditions without ATP and 10% PEG. Topo III was present at a concentration of 0.1 μM , which corresponded to a total of 8 units of topoisomerase activity. For each topoisomerase, 1 activity unit was the amount of protein needed to fully relax 200 ng of pUC19 scDNA in 10 min at 37 °C in 50 μl of the following buffer: 40 mM Na-HEPES (pH 7.5), 1 mM magnesium acetate, 0.1 mg ml^{-1} bovine serum albumin, and 40% glycerol. Unless indicated differently, SSB protein and RPA were present at 0.43 and 0.32 μM , respectively. Aliquots of these reactions were stopped and analyzed by agarose gel electrophoresis as described below.

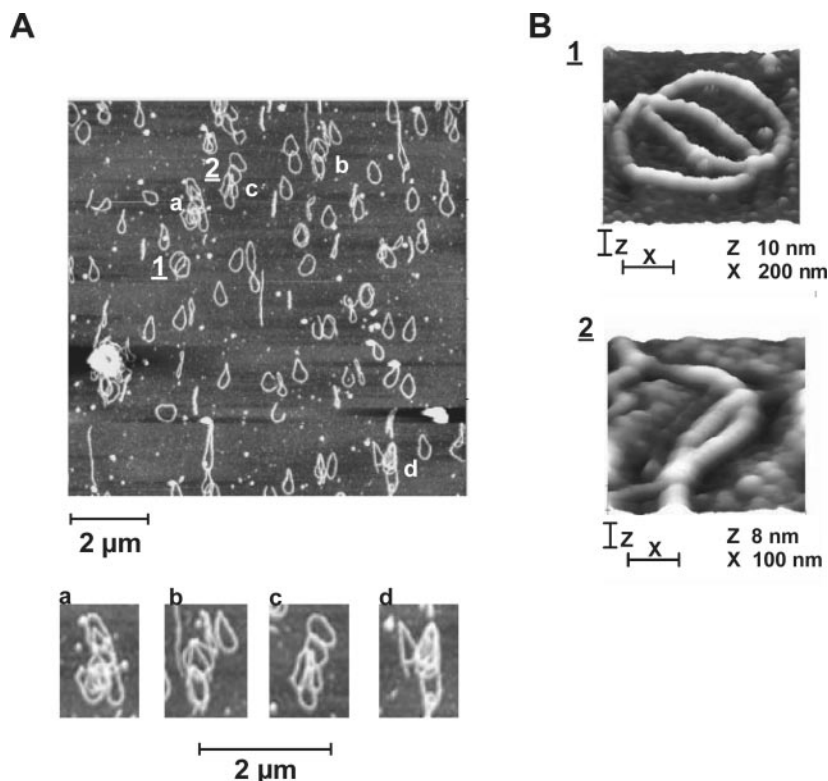
Supercoiling reactions contained 15 μM (nucleotides; 5.6 nM molecules) pUC19 rcDNA, 1.0 μM SSB protein, 1.0 μM RecQ helicase, and 8 units of the indicated topoisomerase. Reactions with wheat germ Topo I were stopped by adding a mix of 5% SDS and 0.25 M EDTA to yield a final concentration of 1% SDS and 50 mM EDTA. The reactions with *E. coli* Topo I and Topo III were stopped by addition of 0.5 M EDTA to a final concentration of 50 mM, followed 2 min later by 10% SDS to a final concentration of 1%. Samples were deproteinized by treatment with 1.5 $\mu\text{g} \mu\text{l}^{-1}$ proteinase K (Roche) at 37 °C for 10 min. pUC19 hdDNA was produced by first incubating a mock reaction lacking proteins at 95 °C for 5 min, then rapidly chilling the sample in an ice water bath for 5 min. Samples were loaded onto a 1% agarose gel, and run in 0.5 \times TBE buffer at 1.5 V cm^{-1} for 12 h. Where indicated, chloroquine diphosphate was present in the gel and running buffer at a concentration of either 0.8 or 8.0 μM . Gels were stained with 1.0 $\mu\text{g} \text{ml}^{-1}$ ethidium bromide in water for 1 h, followed by extensive (>2 h) de-staining with water. Where indicated, gels were dried and probed as described previously (45). The oligonucleotide probe was New England Biolabs M13/pUC19 reverse sequencing primer (-48) that had been 5' end-labeled with [γ - ^{32}P]ATP using T4 polynucleotide kinase. Bands corresponding to DNA were detected using a Storm PhosphorImager (Amersham Biosciences).

Atomic Force Microscopy—Protein-free catenanes were isolated from a standard catenation reaction after 30 min of incubation at 37 °C, followed by deproteinization with proteinase K treatment at 65 °C for 20 min. Proteinase K was inactivated by incubation at 75 °C for 20 min, and the DNA was precipitated with ethanol. The DNA was purified further by use of a MicroSpin S-400 column (Amersham Biosciences). To improve sensitivity, the protein-free catenanes were coated with RecA protein just prior to visualization. The RecA protein-DNA catenane complexes were formed in 50 μl as follows; 5 μM RecA protein was incubated with 66 units of wheat germ Topo I, and \sim 30 μM (nucleotides) DNA products were incubated in 25 mM Na-HEPES (pH 7.5) containing 10 mM magnesium acetate and 2.5 mM ATP at 37 °C for 30 min. ATP γS was then added to a final concentration of 5 mM, and incubation was continued for another 30 min. A 20- μl aliquot of these complexes was then applied to a freshly cleaved mica surface, which was rinsed immediately with 1 ml of water and dried with a stream of nitrogen gas. The sample surface was imaged with a Digital Instruments Nanoscope III in air, using tapping mode with a TESP cantilever. Images were analyzed using Digital Instruments Nanoscope software.

RESULTS

Atomic Force Microscopy Reveals That DNA Catenanes Are Formed by RecQ Helicase and Topo III—Previously, we showed that RecQ helicase and *E. coli* Topo III together comprise a potent DNA strand passage activity, which produces catenated dsDNA (37). In a standard catenation reaction, Topo III and

FIG. 1. The catenanes formed by RecQ helicase and Topo III consist of fully catenated DNA molecules. *A*, a sample of catenanes formed by RecQ helicase and Topo III imaged by AFM contains many linked DNA molecules. To aid visualization, the DNA molecules in the catenane sample were coated with RecA protein. The lowercase letters in the large panel indicate the molecules magnified in the images below, and the numbers correspond to the molecules imaged in *B*. The bar represents 2 μm . *B*, crossover points between fully catenated DNA molecules are clearly discernable for the indicated DNA molecules from *A*. Because AFM provides height information (*Z*), in addition to length and width measurements, each image was rotated backward by 40° in the *X-Y* plane to better display the *Z* dimension.



RecQ helicase (with *E. coli* SSB protein) convert pUC19 scDNA into complex, catenated DNA species (for a representative gel, see Fig. 2, lanes *a-d*). Using restriction analysis, we argued that these complex multimers represented fully catenated DNA (*i.e.* dsDNA molecules linked by a full dsDNA strand pass) rather than hemi-catenated DNA (37).

Both to confirm directly the structure of these multimers and to assess their complexity, protein-free catenanes were imaged by AFM. Visualization was aided by coating the DNA with RecA protein just prior to imaging (46). A representative image, shown at low magnification (10- μm^2 scan area), reveals that RecQ helicase and Topo III form a heterogeneous population of linked DNA molecules (Fig. 1A). The majority of the DNA molecules present are linked with others; of a total of ~80 DNA molecules, ~45 are catenated with one or more DNA molecules. In addition, approximately one-half of the catenanes share multiple points of crossover with the DNA molecules with which they are associated, and the remaining species represent singly linked DNA molecules. The most complex catenated DNA species have a similar makeup; they consist of one primary DNA molecule to which are linked many individual, secondary molecules (Fig. 1A, molecules *a-d*). Linked dsDNA molecules were not observed when a sample of the pUC19 scDNA substrate was imaged using the same procedure (data not shown). The DNA molecules in Fig. 1A that appear as arcs or incomplete circles are not broken DNA molecules but, instead, were not fully coated with RecA protein. At higher magnification, two different catenated DNA species (molecules 1 and 2 in Fig. 1A) show that the path of each individual DNA dsDNA molecule is consistent with a catenated structure (Fig. 1B). This direct analysis complements our previous findings demonstrating that Topo III and RecQ helicase produce fully catenated DNA.

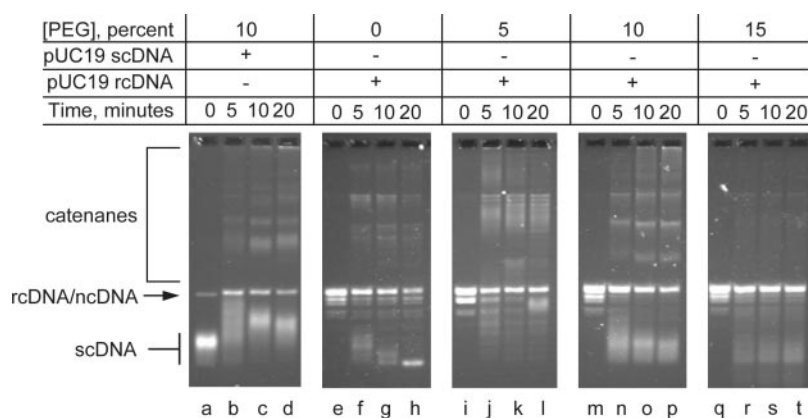
Macromolecular Crowding Favors the Formation of Catenanes by RecQ Helicase and Topo III—To better understand the means by which RecQ helicase and Topo III catenate DNA and to better mimic intracellular conditions, the role of the macromolecular crowding agent, PEG, was determined. The

extent of catenation by RecQ helicase and Topo III could only be measured by quantifying the loss of the initial substrate, because the catenated DNA species are heterogeneous and, therefore, are difficult to quantify directly. However, quantification of the remaining pUC19 scDNA was complicated by the changes in topological state of the uncatenated scDNA substrate during the course of the reaction (Fig. 2, lanes *a-d*). To overcome this problem, rcDNA was used as the starting DNA substrate. Topo III and RecQ helicase readily catenate this DNA substrate in a reaction that is comparable with that observed with pUC19 scDNA (Fig. 2, compare lanes *m-p* with lanes *a-d*). Furthermore, neither RecQ helicase nor Topo III alone produces catenated DNA when provided with this DNA substrate (data not shown), and as seen previously with scDNA (37).

We found that the concentration of PEG has a significant influence on the nature of the DNA species produced by the DNA strand passage activity of RecQ helicase and Topo III (Fig. 2). In the presence of 10% PEG (*i.e.* standard conditions), the reaction is biased toward the production of catenated DNA species, the electrophoretic mobility of which is slower and which accumulate over the 20-min time course (Fig. 2, lanes *m-p*). However, a small proportion of the rcDNA substrate is also converted to faster migrating topological forms. These presumably supercoiled DNA species reach their peak concentration at ~5 min (lane *n*), and their levels do not increase over the remaining 15 min of the reaction.

On the other hand, in the absence of PEG, the bias of the reaction shifted so that RecQ helicase and Topo III mainly change the topology of the individual rcDNA molecules, and produce fewer catenated DNA (Fig. 2, lanes *e-h*). Under these conditions, the majority of the rcDNA substrate is converted to the supercoiled DNA species, which initially are heterogeneous (*i.e.* at 5–10 min) and are subsequently converted into a distinct topological species (lane *h*). The composition of these topological forms is further investigated in a later section (see below). At an intermediate concentration of PEG, 5%, RecQ helicase and Topo III generate an approximately equal mixture of cat-

FIG. 2. Catenation by RecQ helicase and Topo III is enhanced by macromolecular crowding. Reactions were carried out under standard conditions with the indicated concentration of PEG and the following dsDNA substrates: lanes a–d, pUC19 scDNA; lanes e–t, pUC19 rcDNA.



enated and supercoiled products. The putatively supercoiled DNA products migrate more slowly than those produced at either 0 or 10% PEG, which is an indication that RecQ helicase and Topo III introduce smaller changes in the linking number of the rcDNA substrate. Finally, when the PEG concentration was elevated to 15%, catenation was drastically reduced (Fig. 2, lanes q–t) and only a small amount of supercoiled DNA was produced. At an even higher concentration of PEG (20%), the activities of RecQ helicase and Topo III were completely inhibited (data not shown). These results show that PEG is not absolutely required for RecQ helicase and Topo III to exhibit DNA strand passage activity; however, the macromolecular crowding effect of this volume excluding agent does stimulate DNA catenation.

SSB Protein Stimulates DNA Strand Passage Activity by an Effect on the Activity of Topo III—Previously, we demonstrated that the activities of RecQ helicase and Topo III were necessary for DNA strand passage activity (37), but the importance of SSB protein in this activity remained to be determined. Here we show that omission of SSB protein results in lower production of catenated species (Fig. 3, lanes i–l). In addition, the DNA catenanes formed in the absence of SSB protein are less complex, producing fewer discrete species (Fig. 3, compare lanes i–l with lanes m–p).

To determine whether SSB protein is specifically required to stimulate catenation, a heterologous ssDNA-binding protein, the *S. cerevisiae* RPA, was substituted. Replacement of SSB protein with RPA had little overall effect on the conversion of the scDNA substrate to catenated DNA species (Fig. 3). With RPA present, RecQ helicase and Topo III utilized the substrate to the same degree as in the reaction having SSB protein (compare lanes q–t with lanes m–p); in addition, the time required to produce the most complex species was comparable for the two reactions. These results demonstrate that, for optimal DNA strand passage activity, RecQ helicase and Topo III require a ssDNA-binding protein, but this need not be *E. coli* SSB protein.

An obvious means by which a ssDNA-binding protein could promote DNA strand passage is by stimulating RecQ helicase, because the unwinding activity of RecQ helicase is greatly stimulated by ssDNA-binding proteins such as SSB protein and T4 gp32 protein (47, 48). Alternatively, SSB protein and RPA could also affect the activity of Topo III. In support of this latter proposal, the relaxation activity of Topo III is seen to be greater in the presence of SSB protein than in its absence (Fig. 3, compare lanes a–d with lanes e–h); a distribution of topoisomers, which are more relaxed than the pUC19 scDNA substrate (*i.e.* running just above the scDNA), is produced by Topo III in the presence of SSB protein, but not by Topo III alone.

To directly determine the effect of ssDNA-binding proteins on the topoisomerase activity of Topo III in the absence of RecQ

protein, the removal of negative supercoils from a pUC19 scDNA substrate by Topo III was assayed alone and in combination with either SSB protein or RPA (Fig. 4). Topo III alone removed a limited number of supercoils from the substrate over a 10-min time course (Fig. 4A, lanes a–d). On the other hand, Topo III together with either SSB protein or RPA relaxed the scDNA substrate more rapidly and to a greater degree than in their absence (Fig. 4A, lanes e–l). However, the effect of the two ssDNA-binding proteins was not equivalent; Topo III removed supercoils more rapidly in the presence of SSB protein compared with RPA (compare lane f with lane j). Furthermore, the final distribution of topoisomers produced by Topo III in the presence of SSB protein was, on average, more relaxed than that generated by either Topo III alone or Topo III and RPA. These data suggest that SSB protein more effectively stimulates Topo III to relax scDNA than does RPA.

When the topoisomerase activity of Topo III was assayed over a range of SSB protein and RPA stoichiometries, it was clear that SSB protein preferentially stimulates Topo III (Fig. 4B). The concentration of SSB protein and RPA was varied from one-tenth saturating (relative to the total nucleotides of DNA present in the reaction) to fully saturating. The greatest difference between these two proteins was apparent at the 0.1-fold saturating conditions; Topo III relaxed the scDNA to a greater degree in the presence of SSB protein than RPA (Fig. 4B, compare lane c with lane g). The difference was less apparent at the higher concentrations of ssDNA-binding protein. When a saturating amount of ssDNA-binding protein was present (lanes e and i), the final distribution of topoisomers produced by Topo III was essentially equivalent. On the whole, therefore, SSB protein is more effective at stimulating Topo III, but a similar effect is achieved at elevated concentrations of a heterologous ssDNA-binding protein such as RPA.

The Extent of DNA Catenation Is Defined by the RecQ Helicase Concentration, whereas Topo III Primarily Affects the Rate of Catenation—Although the activities of both RecQ helicase and Topo III are required for DNA strand passage activity (37), it was unknown whether optimal activity occurred at a fixed stoichiometry of each protein. To address this question, the effect of protein concentration on DNA catenation was determined by independently varying the concentration of either Topo III or RecQ helicase.

The effect of Topo III concentration on catenation is shown in Fig. 5. Visual inspection of the gels shows that elevation of the topoisomerase concentration leads to an increase in the amount and complexity of catenanes formed in the reaction (Fig. 5A). Because of the complexity of the catenated products, the formation of catenanes was quantified by the rate of utilization/disappearance of the rcDNA substrate. Quantitative analysis of the data in Fig. 5A revealed a hyperbolic dependence on the Topo III concentration (Fig. 5B, squares). The K_{eff} of Topo III

FIG. 3. SSB protein stimulates the DNA strand passage activity of Topo III. Figure shows the effect of either SSB protein or RPA on the catenation of pUC19 scDNA by RecQ helicase and Topo III. Reactions were carried out under standard conditions with SSB protein (1.0 μM) present except for the following: lanes *a-d*, RecQ helicase and SSB protein omitted; lanes *e-h*, RecQ helicase omitted; lanes *i-l*, SSB protein omitted; lanes *q-t*, RPA (0.32 μM) substituted for SSB protein.

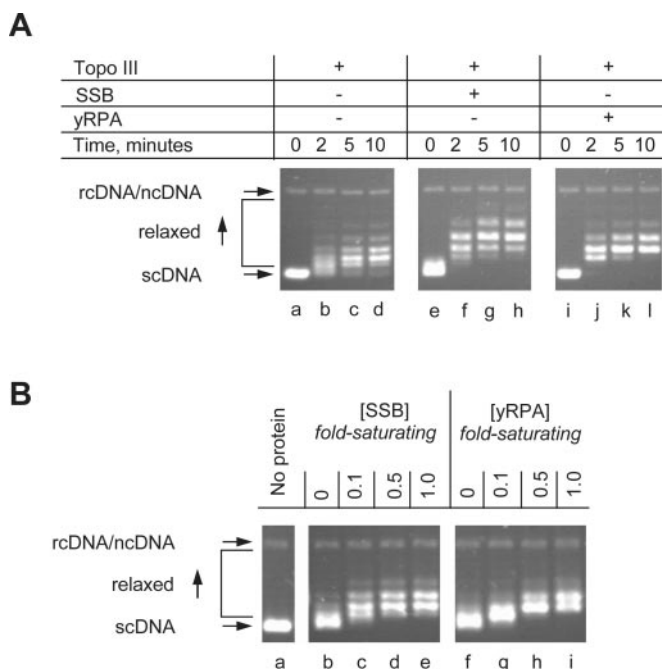
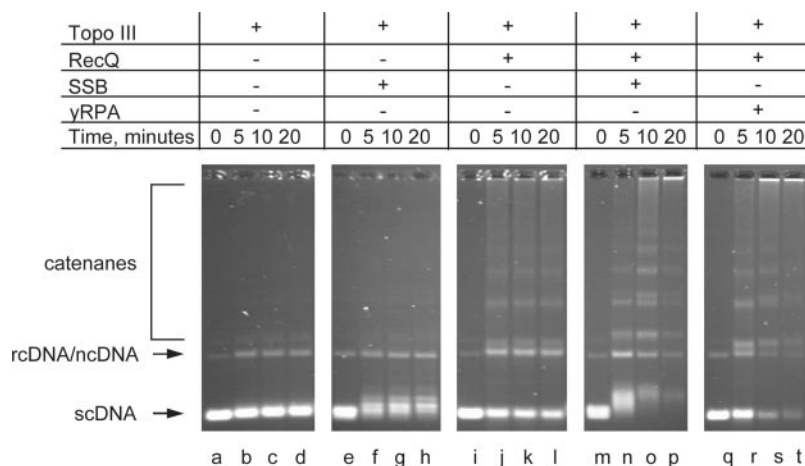


FIG. 4. Topo III relaxes pUC19 scDNA at a higher rate and to a greater extent in the presence of SSB protein. *A*, time course of Topo III-mediated relaxation of pUC19 scDNA. Reactions were carried out under standard conditions without PEG and in the absence (lanes *a-d*) of ssDNA-binding protein or in the presence of either SSB protein (lanes *e-h*) or RPA (lanes *i-l*). Where indicated, SSB protein (0.43 μM) and RPA (0.32 μM) were present at 40% saturation relative to the total concentration of the DNA in nucleotides. *B*, topoisomerase activity of Topo III as a function of the concentration of ssDNA-binding protein. Reactions were carried out under standard conditions with the indicated concentrations of either SSB protein (lanes *b-e*) or RPA (lanes *f-i*). The concentrations of SSB protein and RPA are normalized to the saturating concentration of each protein relative to the DNA substrate, which is 1.0 μM for SSB and 0.75 μM for RPA. Aliquots were taken at 2 min, deproteinized, and analyzed by agarose gel electrophoresis.

and the V_{max} were determined by fitting these data to a rectangular hyperbola (Fig. 5*B*, solid line). The value for the midpoint of the curve, or K_{eff} , was 5.7 ± 1 nM Topo III, and the plateau value, or V_{max} , was $0.62 \pm 0.02\%$ /min.

To determine whether these values were dependent on the concentration of RecQ helicase, the Topo III concentration was varied again, except that the RecQ helicase concentration was 2.5-fold higher at 250 nM (Fig. 5*B*, triangles). The rate of rcDNA utilization displayed a hyperbolic dependence on the concentration of Topo III, and the value for K_{eff} is 9.7 ± 1.2 nM Topo III, which is only 70% greater than that obtained using 2.5-fold less RecQ helicase. However, the higher concentration of RecQ

helicase enabled more rapid utilization of the rcDNA substrate; the V_{max} value was 2.1-fold higher at $1.32 \pm 0.04\%$ /min. The change in the K_{eff} value for Topo III was not directly proportional to the 2.5-fold change in RecQ helicase concentration, implying that complex formation between RecQ helicase and Topo III was not limiting. Rather, the finding that the rate of catenation changed in close proportion to the RecQ helicase concentration suggests that Topo III is acting at a limited number of DNA sites that are "activated" by RecQ helicase and/or by the RecQ-DNA complex itself.

Further elaboration of this finding was provided when we assayed the effect of RecQ helicase concentration on this catenation reaction. Similar to that observed for the topoisomerase concentration dependence, the intensity and complexity of the catenated products increased with RecQ helicase concentration (data not shown). The rate of rcDNA substrate utilization was linear in RecQ helicase concentration over the range that permitted accurate measurements (Fig. 6, squares); linear regression analysis of these data yielded a slope of $0.026 \pm 0.003\%$ /min. To determine whether the rate is affected by Topo III concentration, the effects of RecQ helicase concentration were also examined at 50 nM Topo III (Fig. 6, triangles). These data also conformed to a straight line, and linear regression analysis yielded a slope of $0.030 \pm 0.002\%$ /min. This slope is in close agreement with that calculated for 25 nM Topo III; thus, a 2-fold increase in the concentration of Topo III does not proportionally change the reaction rate. Therefore, in agreement with the data from the topoisomerase concentration dependence, we conclude that the interaction between RecQ helicase and Topo III is not stoichiometric, and that the reaction is limited by the RecQ-DNA complex concentration.

RecQ Helicase and Topo III Convert rcDNA to Denatured rcDNA and Negatively scDNA—The preceding data demonstrate that RecQ helicase and Topo III, acting together, both catenate DNA and introduce topological changes into rcDNA. However, it was not clear whether this second activity produced a supercoiled product that is unique to the DNA strand passage activity of RecQ helicase and Topo III, or whether the products are the result of a DNA helicase unwinding a covalently closed dsDNA substrate in the presence of a topoisomerase. An example of the latter behavior is provided by our previous results for RecQ helicase and wgTopo I; rcDNA unwound by RecQ helicase is converted to negatively scDNA by the topoisomerase activity of wgTopo I (37).

To address the specificity of supercoiling by Topo III and RecQ helicase, we re-examined the production of scDNA from rcDNA by RecQ helicase incubated with Topo III, wgTopo I, or *E. coli* Topo I in the presence of SSB protein (Fig. 7). In all cases, the experiments were carried out in dilute solution (*i.e.*

A

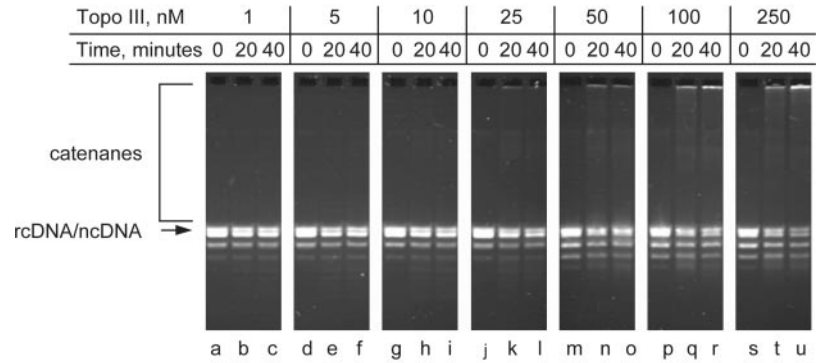


FIG. 5. Effect of Topo III concentration on DNA catenation activity. *A*, catenane formation as a function of the Topo III concentration. Reactions were carried out under standard conditions, except with 100 nM RecQ helicase and the indicated concentration of Topo III. Samples were taken at the indicated time points, deproteinized, and analyzed by agarose gel electrophoresis. *B*, quantitation of the rate of rcDNA substrate utilization as a function of Topo III concentration with either 100 nM (squares, solid line) or 250 nM (triangles, dashed line) RecQ helicase present. Each line corresponds to a fit of the data to a rectangular hyperbola ($Y = V_{\max}(X)/(K_{\text{eff}} + X)$, where V_{\max} is the maximal rate of rcDNA substrate usage, X is the Topo III concentration, and K_{eff} is the Topo III concentration at $0.5V_{\max}$); the R^2 value for each fit was >0.9 .

B

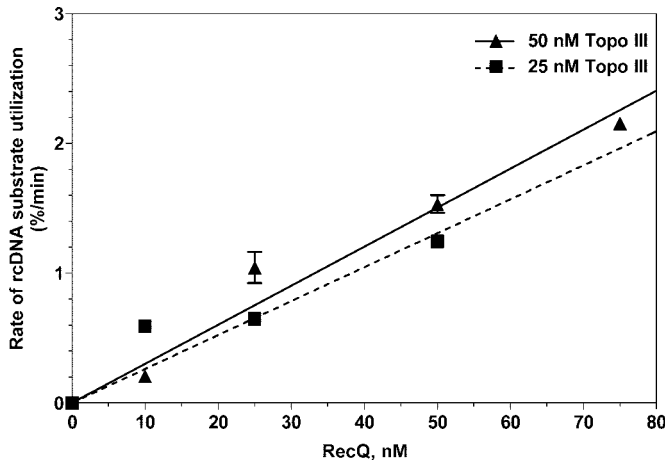
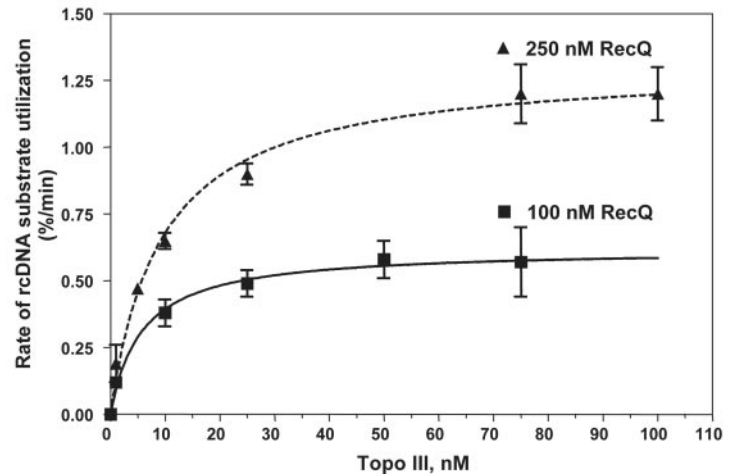


FIG. 6. Effect of RecQ helicase concentration of DNA catenation. Figure shows catenane formation as a function of the RecQ helicase concentration: quantitation of the rate of rcDNA substrate utilization as a function of RecQ helicase concentration with either 25 nM (squares, dotted line) or 50 nM (triangles, solid line) Topo III present. The lines correspond to a fit of the data using linear regression.

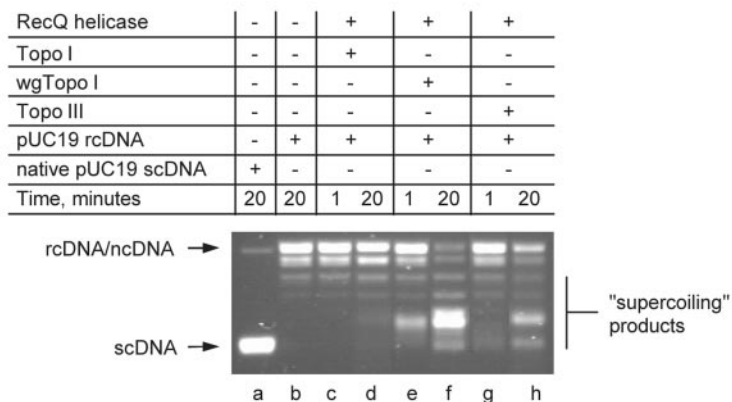
no PEG). Under these conditions, RecQ helicase and Topo III converted the majority of the rcDNA substrate into several distinct DNA species; the species with the fastest mobility appeared within 1 min of initiating the reaction, whereas a slightly slower product was the primary band at 20 min (Fig. 7A, lanes *g* and *h*). Similarly, RecQ helicase and wgTopo I generated several discrete DNA species from the rcDNA substrate (Fig. 7A, lanes *e* and *f*). The most prominent of these

products, which appears to co-migrate with one in the Topo III reaction, appeared early in the reaction and then continued to accumulate over the 20-min time course. In contrast, a combination of RecQ helicase and Topo I had no discernable effect on the migration of the rcDNA substrate (Fig. 7A, lanes *c* and *d*). Furthermore, RecQ helicase alone did not produce comparable DNA species from the rcDNA substrate (data not shown). Thus, Topo III and wgTopo I, but not Topo I, are capable of altering the topology of rcDNA that has been unwound by RecQ helicase.

The preceding data, however, do not distinguish the handedness (*i.e.* positive or negative) of the supercoils introduced into the DNA by the protein combinations. To determine whether the supercoiled products were positively or negatively supercoiled, we used agarose gel electrophoresis in the presence of chloroquine phosphate. The ΔLk of DNA species produced by each helicase-topoisomerase combination was determined by comparing the migration of these species to that of a series of pUC19 scDNA topoisomers (ranging in mean ΔLk value from 0.01 to -8.0) using three separate electrophoresis conditions: the absence of chloroquine, $0.8 \mu\text{M}$ chloroquine, or $8.0 \mu\text{M}$ chloroquine (Fig. 7B, panels 1, 2, and 3, respectively). A grid was used to pinpoint DNA species sharing the same position of migration.

To verify this method, the migration of native pUC19 scDNA topoisomers, which have an average ΔLk value of -6.0 (49), was compared with that of the linking number standards. In agreement with the predicted mean linking number deficit for native scDNA, the band(s) in this DNA sample co-migrated under all three electrophoresis conditions with the bands in the

A



B

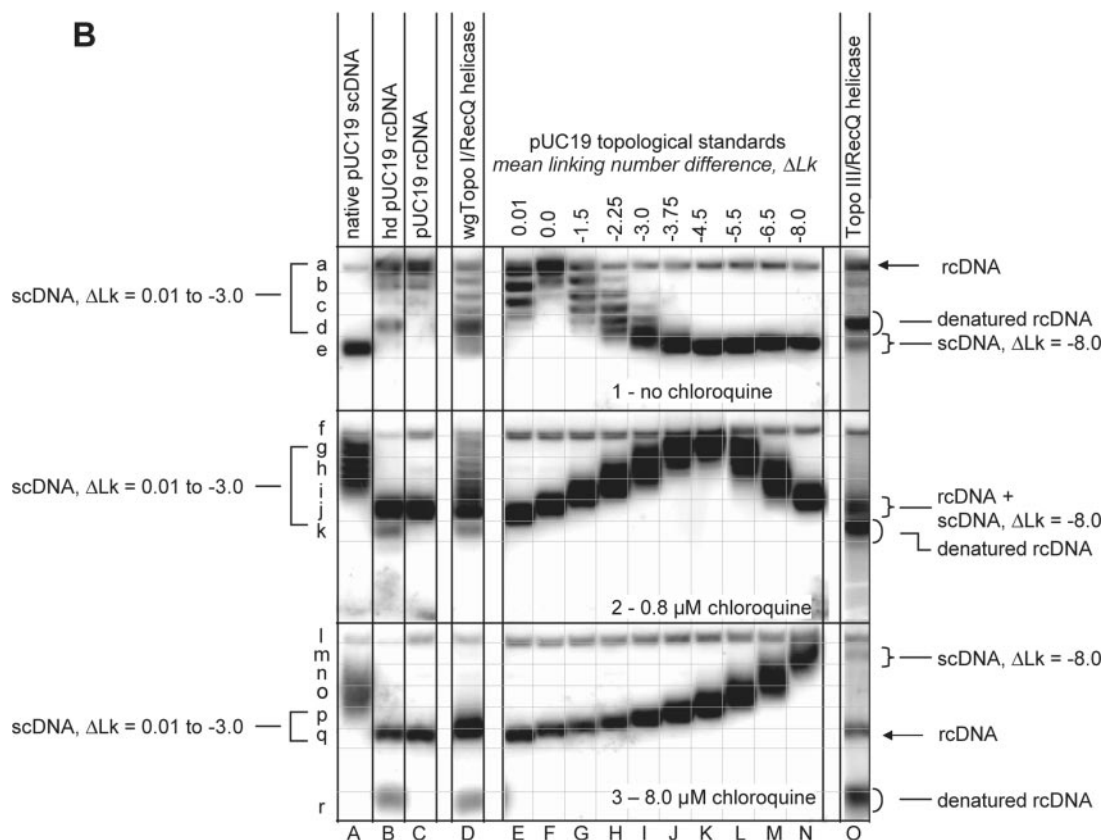


FIG. 7. RecQ helicase and a topoisomerase are capable of removing positive supercoils to produce both denatured DNA and negatively scDNA. A, RecQ helicase at standard conditions was incubated with 8 units of either *E. coli* Topo I (lanes c and d), wheat germ Topo I (lanes e and f), or Topo III (lanes g and h). DNA standards are equivalent amounts of either pUC19 scDNA (lane a) or pUC19 rcDNA (lane b). B, RecQ helicase together with either wgTopo I or Topo III produces both denatured rcDNA and scDNA. Samples of the DNA products produced at 20 min by RecQ helicase and either wgTopo I (lane D) or Topo III (lane O) from the reactions shown in A were analyzed separately by agarose gel electrophoresis in buffer supplemented as indicated: no chloroquine, panel 1 (rows a–e); 0.8 μM chloroquine, panel 2 (rows f–k); and 8.0 μM chloroquine, panel 3 (rows l–r). Lanes A–C were loaded with either pUC19 scDNA, hddDNA, or pUC19 rcDNA, respectively. Lanes E–N contained pUC19 topological standards, and each lane was loaded with a set of topoisomers having the mean ΔLk value indicated above the lane (extending from 0.01 to -8.0). Markers to the left indicate the position of the major products of the reaction with RecQ helicase and wgTopo I: *l*, negatively scDNA with a ΔLk value between 0.01 and -3.0 ; *;*, denatured rcDNA. Markers to the right indicate the position of the major products of the reaction with RecQ helicase and Topo III: *j*, negatively scDNA with a mean ΔLk value of -8.0 ; and *),* denatured rcDNA. DNA species were detected by autoradiography following probing of the dried gels with a ^{32}P -labeled oligonucleotide probe. The samples in each panel were analyzed on the same gel; however, the position of lanes D and O were shifted for clarity of presentation.

topoisomer groups having an average ΔLk of -5.5 and -6.5 (Fig. 7B, compare lane A with lanes L and M, rows e, g, and h, and rows n and o). Additional standards on all three gels were

the starting pUC19 rcDNA substrate (lane C) and hddDNA (lane B). The latter was included as a migration standard for the unwinding products of RecQ helicase. Heat treatment of

rcDNA produced a novel band that was absent from the rcDNA sample (compare lanes B and C, row d; molecules indicated by the λ symbol to the right), and this DNA species migrated ahead of all the topological standards under both chloroquine conditions (rows k and r), consistent with this band representing either fully or partially denatured rcDNA.

Samples collected at 20 min from the reactions described in Fig. 7A were subjected to the electrophoresis conditions described above (Fig. 7B). As expected, RecQ helicase, SSB protein, and wgTopo I together convert pUC19 rcDNA to faster migrating DNA species (lane D, rows c–e; products indicated by the λ symbol to left). The migration of the bulk of the DNA species produced by these two proteins mirrors that of the topological standards with ΔLk values ranging from ~ 0.01 to -3.0 (compare lane D with lanes G–L, rows c–e, h–j, and p–q; the area indicated by the λ symbol to the left). Thus, the major product of RecQ helicase and wgTopo I is a distribution of slightly negatively scDNA. These findings are consistent with our previous results demonstrating that RecQ helicase and wgTopo I introduce negative supercoils into rcDNA by relaxing the free positive supercoils (the negative supercoils are the unwound regions that are bound and stabilized by the SSB and RecQ proteins) (37).

Similarly, a combination of RecQ helicase and Topo III produces a distribution of faster migrating DNA species comparable with what is produced in the presence of wgTopo I (compare lanes D and O, rows d and e; molecules indicated by the λ and μ symbols to the right). In this case, however, the major product of the reaction appears to be denatured rcDNA; under all three electrophoresis conditions, the prominent band produced by RecQ helicase and Topo III co-migrates with the band in the hdDNA sample corresponding to denatured products (compare lanes B and O, rows d, k, and r; indicated by the λ symbol to the right). This reaction also produced a dsDNA species that is highly negatively scDNA. This band, which corresponds to the faster migrating species observed in the absence of chloroquine, co-migrates under all three electrophoresis conditions with the group of topoisomers having a ΔLk of -8.0 (compare lanes N and O, rows e, i, j, and m; areas indicated by the λ symbol at the right). Clearly, a combination of RecQ helicase and either Topo III or wheat germ Topo I introduces negative supercoils into rcDNA; thus, these products appear to be general result of unwinding a covalently closed dsDNA substrate in the presence of a topoisomerase. Nevertheless, this finding implies that Topo III and wgTopo I are selectively removing positive supercoils introduced into the DNA molecule by RecQ helicase-mediated unwinding. Because Topo III and RecQ helicase both introduce a greater linking number change in the DNA substrate and produce more denatured rcDNA product, the two *E. coli* proteins together appear to possess more positive supercoil removal activity compared with the heterologous reaction with wgTopo I.

DISCUSSION

Previously, we demonstrated that RecQ helicase and Topo III together comprise a potent DNA strand passage activity that can catenate and decatenate covalently closed dsDNA (37). Here we directly visualized protein-free catenanes using AFM, which revealed that the individual dsDNA molecules incorporated into catenanes are linked together by intact dsDNA strands and, therefore, constitute full catenanes. RecQ helicase and Topo III can not only catenate/decatenate DNA, they also can change the topological state of dsDNA by altering the linking number of individual molecules. Macromolecular crowding (achieved by use of PEG) influenced the distribution of products that were formed; at high PEG concentrations, catenated DNA was the major product, whereas at low concen-

trations, denatured DNA and highly negatively scDNA were predominant products. SSB protein greatly stimulated the DNA strand passage activity of RecQ helicase and Topo III, and it stimulated the topoisomerase activity of Topo III. An examination of the effects of both RecQ helicase and Topo III concentration on DNA strand passage revealed that stoichiometric complex formation between these two proteins was not occurring; however, the results revealed that the likely target for Topo III action was a limiting amount of RecQ helicase bound to the site of strand passage.

The model in Fig. 8 illustrates the DNA strand passage activity of RecQ helicase and Topo III in the context of dilute and volume-excluded reaction conditions. We propose that both the catenation and the supercoiling activities exhibited by the combined activities of these proteins arise from the same mechanism, namely two concerted single DNA strand passage events. Initially, the dsDNA is unwound by RecQ helicase to produce ssDNA, which is subsequently bound by SSB protein. The binding of SSB protein to the ssDNA product of RecQ helicase both prevents the individual ssDNA strands from reannealing (48, 50) and, based on the data presented here, possibly directs the binding of Topo III to regions of DNA where a limited number of RecQ helicase molecules are acting (*i.e.* the unwinding fork). Because of the specificity of the catenation reaction (37), Topo III must also recognize a particular aspect of the RecQ helicase-ssDNA product complex that stimulates its DNA strand passage activity. Once Topo III gains access to the ssDNA substrate, it mediates the passage of one strand of the unwound region across an intact duplex region to produce a hemi-catenane. A second single-strand passage event with the opposite unwound strand achieves full catenation of the second molecule. Interestingly, *Drosophila* topoisomerase III β has recently been shown to produce reversible double-stranded DNA breaks (51), which is the type of activity needed to achieve a catenation reaction comparable with that we observe for the *E. coli* proteins.

The role of macromolecular crowding is to alter the bias of each reaction shown in Fig. 8: intermolecular *versus* intramolecular. Under volume excluded conditions, (*i.e.* the presence of 10% PEG), the preferred reaction is an intermolecular DNA strand passage event that catenates a second, duplex DNA molecule to produce fully catenated dsDNA molecules (Fig. 8A). The macromolecular crowding effect of PEG most likely stimulates catenation by establishing a high local concentration of the DNA substrate, thereby bringing substrate molecules together to enhance catenation. AFM imaging revealed that the catenated products are an almost equal mix of singly catenated DNA molecules and multiply linked DNA molecules. The majority of the multiply catenated DNA species are similar in their structure; several individual, secondary molecules are catenated with one, apparently primary, DNA molecule in a key ringlike structure. These catenanes most likely arose from a series of sequential catenation events carried out by a single Topo III complex bound at one position to the primary molecule in a gating type of reaction. These data suggest that Topo III remains bound to a single position on a DNA substrate for a relatively long period of time.

On the other hand, the predominant activity exhibited by RecQ helicase and Topo III in dilute solution conditions is to alter the linking number of individual DNA substrates (Fig. 8B). A primary product of this activity is negatively supercoiled DNA (see below); thus, Topo III is selectively removing the positive supercoils introduced into the covalently closed dsDNA by the helicase activity of RecQ helicase. The expected mechanism for this activity is two sequential intramolecular DNA strand passage events, mediated by Topo III acting on the

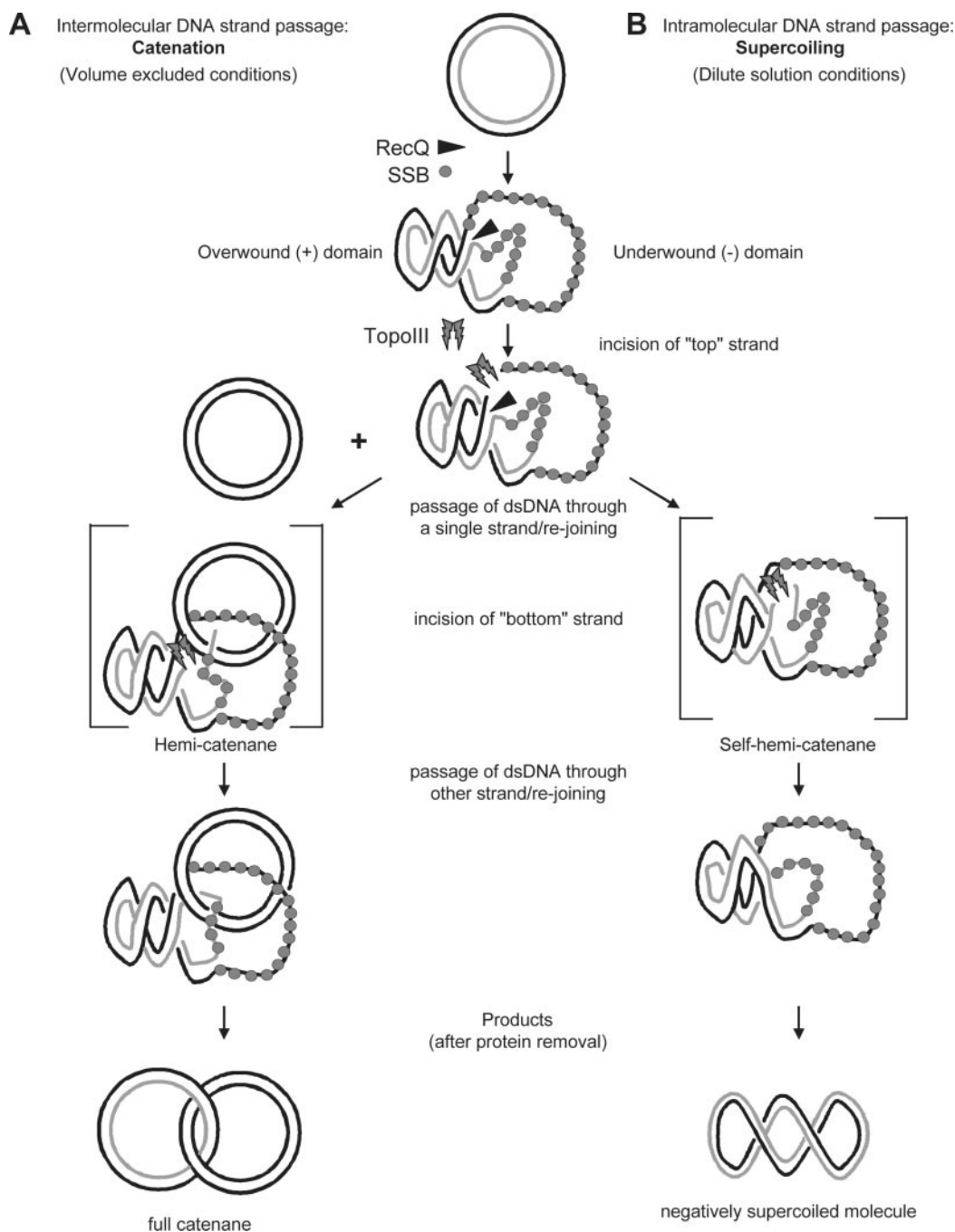


FIG. 8. **The DNA strand passage activity of RecQ helicase and Topo III can both catenate and supercoil DNA.** *A*, intermolecular DNA strand passage. RecQ helicase and Topo III can mediate the full catenation of two dsDNA molecules; this process is preferred at high DNA concentrations (*e.g.* in the presence of a volume exclusion agent). *B*, intramolecular DNA strand passage. RecQ helicase and Topo III can remove positive supercoils when the DNA concentration is low. Note that the catalytic mechanism in both cases is identical, and the only difference is whether DNA strand passage occurs with a different DNA molecule intermolecularly, or with the same DNA molecule intramolecularly. See "Discussion" for details.

single-stranded regions at or just behind the point of unwinding, that decatenate the accumulated regions of positive writhe. Consistent with this proposal, Topo III also allows replication of covalently closed plasmid DNA *in vitro* by removing positive supercoils generated by the replication fork (40). After removal of the positive supercoils by the topoisomerase, the negative supercoils remain in the closed DNA molecules because SSB protein prevents reannealing of the individual ssDNA strands unwound by RecQ helicase. As a result, the combined functions of RecQ helicase, Topo III, and SSB protein result in a net accumulation of negative supercoils. This mechanism of action for Topo III is in contrast to that expected for

the nonspecific reaction with wgTopoI, where this type IB topoisomerase (*i.e.* binds to dsDNA and cleaves a single strand) most likely removes positive supercoils by acting on the double-stranded regions of the substrate molecule away from the unwinding fork.

Quantitative analysis of the supercoiled products formed by RecQ helicase and Topo III indicated that these molecules had a ΔLk value of approximately -8.0 to mostly denatured rcDNA. Negatively supercoiled DNA was also produced by RecQ helicase and wgTopoI; however, the linking number of the final products was significantly higher. A combination of RecQ and wgTopoI produced scDNA primarily with a ΔLk value no

smaller than -3.0 and some denatured rcDNA. The production of both denatured rcDNA and negatively scDNA in both cases argues that these products are the result of removal of the positive supercoils introduced into the covalently closed DNA substrate by RecQ helicase-mediated unwinding. The fact that the DNA strand passage activity of RecQ helicase and Topo III produces more highly negatively supercoiled DNA and a larger proportion of denatured rcDNA, compared with the heterologous reaction with wgTopo I, suggests that the *E. coli* proteins possess more positive supercoil removal activity. This activity is specific for *E. coli* Topo III, in that neither *E. coli* Topo I, Topo II, nor Topo IV is stimulated by RecQ helicase (37). Thus, of the *E. coli* topoisomerases tested, only Topo III is activated by RecQ helicase.

SSB protein had a significant, positive influence on the yield of catenanes produced by RecQ helicase and Topo III. When SSB protein was present, RecQ helicase and Topo III utilized the scDNA substrate to a greater extent and the resultant catenanes were more complex. The most direct means by which single-stranded DNA-binding proteins can affect DNA strand passage is via the helicase activity of RecQ helicase. SSB protein is an important stimulatory cofactor for the unwinding activity of RecQ helicase; both the rate and extent of dsDNA unwinding are significantly increased in the presence of SSB protein (47, 48). Because the catenation activity of RecQ helicase and Topo III is dependent on the unwinding activity of RecQ helicase (37), the positive effect of SSB protein is likely the result of a stimulation of DNA unwinding by RecQ helicase. In agreement with these findings, the stimulatory effect of BLM helicase on the DNA strand passage activity of hTopo III α is dependent upon the presence of a single-stranded binding protein (38).

Although the role of SSB protein outlined above is plausible, we also explored the additional possibility that ssDNA-binding proteins stimulated the activity of Topo III itself. In agreement, we found that Topo III relaxed a scDNA substrate more quickly and with a higher average change in linking number in the presence of ssDNA-binding proteins. However, the effect of SSB protein and RPA was not the same; SSB protein was consistently a more effective stimulator than RPA, except at saturation. SSB protein allowed Topo III to relax a scDNA substrate more rapidly and with a greater degree of relaxation than did the equivalent concentration of RPA, suggesting a limited degree of specificity for SSB protein. A potential mechanism for stimulation of Topo III by SSB protein is through the trapping of transient ssDNA in negatively supercoiled DNA; SSB protein would trap the DNA species that is the preferential substrate for Topo III binding (33), thereby allowing the topoisomerase access to the DNA. Another Topo III-like topoisomerase, hTopo III α , is also stimulated by a single-stranded DNA-binding protein; the rate and extent of relaxation of negatively scDNA by hTopo III α is elevated in the presence of either *E. coli* SSB protein or hRPA (38).

The dependence of RecQ helicase and Topo III concentration on DNA strand passage revealed that optimal catenation does not require a fixed stoichiometry of these two proteins relative to one another. However, the rate of catenation was dependent upon the concentration of Topo III, whereas the extent of catenation was defined by the concentration of RecQ helicase. These results support our previous model for catenation, in which we proposed that Topo III was possibly targeted to the DNA by the DNA structure formed by the RecQ helicase-unwinding complex. We suggest that the DNA unwinding fork, with RecQ at the junction and SSB protein bound to the unwound ssDNA regions, is the likely site. Thus, we imagine that at least a subset of cellular sites of action for Topo III are the

same sites at which RecQ helicase, and some of the RecQ-homologues, can act, namely recombination intermediates and stalled replication forks. Direct protein-protein interactions are likely to be important for the coordinated action of the RecQ helicase homologues and Topo III. In support of this view, the DNA strand passage activity of hTopo III α is stimulated by the human BLM helicase, but only if the two proteins are capable of physical interaction (38).

Recent work in *E. coli* supports the idea that Topo III is needed *in vivo* to decatenate chromosomes, particularly those that are linked following homologous recombination. Cells lacking both Topo I (*topA*) and Topo III (*topB*) activity have a chromosome partitioning defect (a *par* phenotype, where filamented cells appear that are unable to segregate their chromosomes), which is not caused by SOS induction (52). Interestingly, this phenotype is suppressed by a *recA* mutation. Furthermore, a *topArecQ* deletion strain has a comparable chromosomal segregation defect, which suggests that Topo III and RecQ helicase act together to eliminate crossovers generated by homologous recombination. This function appears to be specific to Topo III, because the *par* phenotype in cells lacking *topA* and *topB* is not rescued by overexpression of Topo IV, which is the archetypal decatenase in *E. coli*. The authors' interpretation of the data is that either Topo I or Topo III is needed to allow resolution of Holliday junctions around which replication-induced strand "interlinks" have accumulated. In this model, a significant proportion of the proposed interlinks within the arms of the Holliday junction should consist of positive supercoiled regions; Topo III, alone, cannot act on such a substrate, but when combined with RecQ helicase, our work shows that both relaxation and decatenation are possible.

Further support for the proposal that Topo III is also an important cellular decatenase is the finding that Topo III is a high copy number suppressor of the growth and chromosome segregation defects observed at non-permissive temperatures in temperature-sensitive alleles of *parC* and *parE* (the genes that encode the subunits of Topo IV) (53). Topo III appears to accomplish this task by decatenating precatenanes (positive supercoils that have equalized across the replication fork to intertwine the two daughter duplexes) that accumulate behind the replication fork as DNA replication nears completion. However, in this case, a *recQ* mutation does not diminish the rescue of a *parE* temperature-sensitive strain by the high levels of Topo III. This absence of a *recQ* dependence may either be a consequence of the overproduction of Topo III (perhaps because of competition for a limited number of ssDNA sites), or signify that Topo III does not require its partnership with RecQ helicase to achieve the removal of precatenanes. Therefore, it is simplest to imagine that the site of action for Topo III is a region of ssDNA proximal to the replication fork, either between Okazaki fragments or just behind the replication apparatus. In the absence of such preexisting ssDNA sites for Topo III binding, decatenation would require the combined actions of Topo III and RecQ helicase. Thus, the activity of Topo III alone may be sufficient when ssDNA exists at sites, such as replication forks, but the combined activity of RecQ helicase and Topo III is required when the DNA is duplex or topologically hindered, such as at Holliday junction recombination intermediates. Consequently, it is clear that Topo III is a chromosomal decatenase, and that this function is mediated, in part, by the DNA strand passage activity resulting from its interaction with RecQ helicase.

REFERENCES

1. Karow, J. K., Wu, L., and Hickson, I. D. (2000) *Curr. Opin. Genet. Dev.* **10**, 32-38
2. Irino, N., Nakayama, K., and Nakayama, H. (1986) *Mol. Gen. Genet.* **205**, 298-304

3. Gangloff, S., McDonald, J. P., Bendixen, C., Arthur, L., and Rothstein, R. (1994) *Mol. Cell. Biol.* **14**, 8391–8398
4. Watt, P. M., Louis, E. J., Borts, R. H., and Hickson, I. D. (1995) *Cell* **81**, 253–260
5. Stewart, E., Chapman, C. R., Al-Khodairy, F., Carr, A. M., and Enoch, T. (1997) *EMBO J.* **16**, 2682–2692
6. Cogoni, C., and Macino, G. (1999) *Science* **286**, 2342–2344
7. Kusano, K., Berres, M. E., and Engels, W. R. (1999) *Genetics* **151**, 1027–1039
8. Yan, H., Chen, C. Y., Kobayashi, R., and Newport, J. (1998) *Nat. Genet.* **19**, 375–378
9. Puranam, K. L., and Blackshear, P. J. (1994) *J. Biol. Chem.* **269**, 29838–29845
10. Ellis, N. A., Groden, J., Ye, T. Z., Straughen, J., Lennon, D. J., Ciocci, S., Proytcheva, M., and German, J. (1995) *Cell* **83**, 655–666
11. Yu, C. E., Oshima, J., Fu, Y. H., Wijsman, E. M., Hisama, F., Alisch, R., Matthews, S., Nakura, J., Miki, T., Ouais, S., Martin, G. M., Mulligan, J., and Schellenberg, G. D. (1996) *Science* **272**, 258–262
12. Kitao, S., Shimamoto, A., Goto, M., Miller, R. W., Smithson, W. A., Lindor, N. M., and Furuichi, Y. (1999) *Nat. Genet.* **22**, 82–84
13. Gorbalenya, A. E., Koonin, E. V., Donchenko, A. P., and Blinov, V. M. (1989) *Nucleic Acids Res.* **17**, 4713–4730
14. Umezu, K., Nakayama, K., and Nakayama, H. (1990) *Proc. Natl. Acad. Sci. U. S. A.* **87**, 5363–5367
15. Gray, M. D., Shen, J. C., Kamath-Loeb, A. S., Blank, A., Sopher, B. L., Martin, G. M., Oshima, J., and Loeb, L. A. (1997) *Nat. Genet.* **17**, 100–103
16. Karow, J. K., Chakraverty, R. K., and Hickson, I. D. (1997) *J. Biol. Chem.* **272**, 30611–30614
17. Bennett, R. J., Sharp, J. A., and Wang, J. C. (1998) *J. Biol. Chem.* **273**, 9644–9650
18. Lindor, N. M., Furuichi, Y., Kitao, S., Shimamoto, A., Arndt, C., and Jalal, S. (2000) *Am. J. Med. Genet.* **90**, 223–228
19. Chakraverty, R. K., and Hickson, I. D. (1999) *BioEssays* **21**, 286–294
20. German, J. (1993) *Medicine* **72**, 393–406
21. Sinclair, D. A., Mills, K., and Guarente, L. (1997) *Science* **277**, 1313–1316
22. Sinclair, D. A., Mills, K., and Guarente, L. (1998) *Trends Biochem. Sci.* **23**, 131–134
23. Hanada, K., Ukita, T., Kohno, Y., Saito, K., Kato, J., and Ikeda, H. (1997) *Proc. Natl. Acad. Sci. U. S. A.* **94**, 3860–3865
24. Hanai, R., Caron, P. R., and Wang, J. C. (1996) *Proc. Natl. Acad. Sci. U. S. A.* **93**, 3653–3657
25. Ng, S. W., Liu, Y., Hasselblatt, K. T., Mok, S. C., and Berkowitz, R. S. (1999) *Nucleic Acids Res.* **27**, 993–1000
26. Li, W., and Wang, J. C. (1998) *Proc. Natl. Acad. Sci. U. S. A.* **95**, 1010–1013
27. Wallis, J. W., Chrebet, G., Brodsky, G., Rolfe, M., and Rothstein, R. (1989) *Cell* **58**, 409–419
28. DiGate, R. J., and Mariani, K. J. (1989) *J. Biol. Chem.* **264**, 17924–17930
29. Goodwin, A., Wang, S. W., Toda, T., Norbury, C., and Hickson, I. D. (1999) *Nucleic Acids Res.* **27**, 4050–4058
30. Maftahi, M., Han, C., Langston, L. D., Hope, J. C., Zigouras, N., and Freyer, G. A. (1999) *Nucleic Acids Res.* **27**, 4715–4724
31. Whoriskey, S. K., Schofield, M. A., and Miller, J. H. (1991) *Genetics* **127**, 21–30
32. Schofield, M. A., Agbunag, R., Michaels, M. L., and Miller, J. H. (1992) *J. Bacteriol.* **174**, 5168–5170
33. DiGate, R. J., and Mariani, K. J. (1988) *J. Biol. Chem.* **263**, 13366–13373
34. Kim, R. A., and Wang, J. C. (1992) *J. Biol. Chem.* **267**, 17178–17185
35. Bennett, R. J., Noiro-Gros, M.-F., and Wang, J. C. (2000) *J. Biol. Chem.* **275**, 26898–26905
36. Wu, L., Davies, S. L., North, P. S., Goulaouic, H., Riou, J. F., Turley, H., Gatter, K. C., and Hickson, I. D. (2000) *J. Biol. Chem.* **275**, 9636–9644
37. Harmon, F. G., DiGate, R. J., and Kowalczykowski, S. C. (1999) *Mol. Cell* **3**, 611–620
38. Wu, L., and Hickson, I. D. (2002) *Nucleic Acids Res.* **30**, 4823–4829
39. Harmon, F. G., and Kowalczykowski, S. C. (1998) *Genes Dev.* **12**, 1134–1144
40. Hiasa, H., and Mariani, K. J. (1994) *J. Biol. Chem.* **269**, 32655–32659
41. LeBowitz, J. (1985) *Biochemical Mechanism of Strand Initiation in Bacteriophage Lambda DNA Replication*. Ph.D. thesis, Johns Hopkins University, Baltimore, MD
42. Harmon, F. G., Rehrauer, W. M., and Kowalczykowski, S. C. (1996) *J. Biol. Chem.* **271**, 23874–23883
43. Sambrook, J., Fritsch, E. F., and Maniatis, T. (1989) *Molecular Cloning: A Laboratory Manual*, 2nd Ed., Cold Spring Harbor Laboratory Press, Cold Spring Harbor, NY
44. Bowater, R., Aboul-Ela, F., and Lilley, D. M. J. (1992) *Methods Enzymol.* **212**, 105–120
45. Zerbib, D., Colloms, S. D., Sherratt, D. J., and West, S. C. (1997) *J. Mol. Biol.* **270**, 663–673
46. Krasnow, M. A., Stasiak, A., Spengler, S. J., Dean, F., Koller, T., and Cozzarelli, N. R. (1983) *Nature* **304**, 559–560
47. Umezu, K., and Nakayama, H. (1993) *J. Mol. Biol.* **230**, 1145–1150
48. Harmon, F. G., and Kowalczykowski, S. C. (2001) *J. Biol. Chem.* **276**, 232–243
49. Hanai, R., and Roca, J. (2000) *Methods Mol. Biol.* **94**, 19–26
50. Roman, L. J., and Kowalczykowski, S. C. (1989) *Biochemistry* **28**, 2863–2873
51. Wilson-Sali, T., and Hsieh, T. S. (2002) *J. Biol. Chem.* **277**, 26865–26871
52. Zhu, Q., Pongpech, P., and DiGate, R. J. (2001) *Proc. Natl. Acad. Sci. U. S. A.* **98**, 9766–9771
53. Nurse, P., Levine, C., Hassing, H., and Mariani, K. J. (2003) *J. Biol. Chem.* **278**, 8653–8660